

doi:10.15199/48.2024.07.08

Comparative analysis of the 4-pole and 8-pole radial magnetic bearings with permanent magnets

Abstract. This paper presents a comparison of two constructions of radial magnetic bearings with permanent magnets. The first construction has four poles with coils and four permanent magnets installed in the stator yoke. The second construction has eight poles, four poles with coils and four poles with installed permanent magnets. Both constructions have two control windings, one for the x-axis and the second for the y-axis, that allow controlling the magnetic force generated by the magnetic bearing. Comparative analysis takes into account parameters of the magnetic bearing like the position and current stiffness, the maximal and initial magnetic forces as well as the dynamic inductances and the velocity-induced voltages.

Streszczenie. W artykule przedstawiono porównanie dwóch konstrukcji radialnych łożysk magnetycznych z magnesami trwałymi. Pierwsza konstrukcja ma cztery nabiegunki z nawiniętymi cewkami oraz cztery magnesy trwałe zainstalowane w jarmie stojana. Druga konstrukcja ma osiem nabiegunków, z czego cztery nabiegunki mają nawinięte cewki oraz w kojonych czterech nabiegunkach umieszczone są magnesy trwałe. Obie konstrukcje mają dwa uzwojenia sterujące, jedno dla osi x oraz drugie dla osi y, które umożliwiają sterowanie siłą magnetyczną generowaną przez łożysko magnetyczne. Analiza porównawcza obejmuje parametry łożyska magnetycznego takie jak sztywność przemieszczeniowa i prądowa, maksymalną i początkową siłę magnetyczną jak również dynamiczną indukcyjność oraz napięcie indukowane w wyniku przesunięcia wirnika. (Analiza porównawcza 4-biegunowych i 8-biegunowych promieniowych łożysk magnetycznych z magnesami trwałymi)

Keywords: radial magnetic bearing, permanent magnets, finite element model, parameters of the magnetic bearings

Słowa kluczowe: radialne łożysko magnetyczne, magnesy trwałe, model na podstawie metody elementów skończonych, parametry łożysk magnetycznych

Introduction

A magnetic bearing is a special type of electric machine that uses a magnetic field to levitate the rotor without mechanical contact. This feature causes magnetic bearings to have a few significant and unique advantages, like:

- high rotational speed,
- high lifetime,
- operation without lubrication,
- operation in a vacuum, in a clean/harsh environment, in a wide range of temperatures,
- compensation of the unbalanced forces and/or external forces,
- precise controlling of the rotor position in active magnetic bearings.

Magnetic bearings have also disadvantages:

- active magnetic bearings require a complicated control system with proximity sensors,
- in active magnetic bearings, the rotor has to be made of ferromagnetic material,
- passive magnetic bearings have a low damping factor.

Magnetic bearings are used in many industrial applications such as flywheel energy storages, electrospindles, high-speed motors, blowers, blood pumps, active magnetic dampers, turbo generators, drives of hard discs and wind generators [1, 2].

Magnetic bearings can be categorised according to various classifications. One categorization classifies them as radial and axial magnetic bearings, used for levitation of the rotor in the radial and axial direction, respectively [3]. The second categorization classifies magnetic bearings as active magnetic bearings [1], passive magnetic bearings [4, 5] and active magnetic bearings with permanent magnets, sometimes called hybrid magnetic bearings [6]. Active magnetic bearings use a control system for the stabilization of the rotor position, which modifies currents excited in windings based on the position of the rotor. Passive magnetic bearings use a combination of permanent magnets to create repulsive force. Unfortunately, it is impossible to use all passive magnetic bearings for the rotor levitation in an electric machine. Therefore, at least one axis must be actively stabilized or another type of bearing must be installed. Active magnetic bearings with permanent

magnets use a control system for the stabilization of the rotor position and permanent magnets for the generation of the bias flux. The bias flux is used for the pre-magnetization of the magnetic circuit of the magnetic bearing so that it is possible to control the magnetic force generated by the magnetic bearing. The usage of permanent magnets increases the efficiency of the magnetic bearing. Therefore, in recent years, it can be seen an increase in research activity concerning magnetic bearings with permanent magnets [7, 8, 9, 10].

This paper aims to present a comparison of two variants of magnetic bearings with permanent magnets. The comparative analysis takes into account the parameters of the magnetic bearings like the position and current stiffness, the maximal and initial magnetic forces as well as the dynamic inductances and the velocity-induced voltages. The main difference between the presented magnetic bearings is that the first variant has four permanent magnets installed in the stator yoke, while the second variant has four permanent magnets installed in the poles of the stator.

Previously, the author of this paper published a work concerning the comparison of two variants of the 6-pole magnetic bearings with permanent magnets [6]. Therefore, this paper enhances the previous work and presents another two variants of radial magnetic bearings with permanent magnets.

Construction of the 4-pole and 8-pole radial magnetic bearings with permanent magnets

Two versions of the magnetic bearings were analysed in this paper. For both versions, a stator and rotor are made of the dynamo steel sheet M400-50A, which is 0.5 mm thick. Fig. 1 presents the $B-H$ curve of this magnetic material measured with a closed magnetic circuit method [11].

The 4-pole and 8-pole magnetic bearings have four poles with coils. The number of turns for one coil of the 4-pole magnetic bearing equals 200, while for the 8-pole magnetic bearing equals 75. The number of turns was customized to obtain the same range of the control current for both versions. Two opposite coils are connected in series to create one winding, that controls the position of

the rotor along one axis. Analysed versions of the magnetic bearings have two windings, the first one controls the position of the rotor along the x -axis and the second one controls the position of the rotor along the y -axis. The control currents for both versions can change within the range -2 A to 2 A. Whereas, the rotor position can change within the range -0.2 mm to 0.2 mm, while the air gap between the stator and rotor equals 0.3 mm. The movement of the rotor must be limited to protect the rotor against destruction by hitting the stator. Most often this limitation of the rotor movement is done by the installation of the auxiliary mechanical bearing [12].

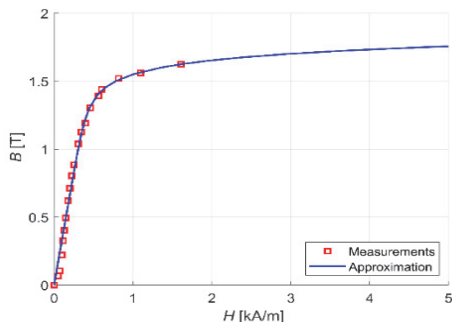


Fig. 1. The B - H curve of the M400-50A silicon steel

The 4-pole magnetic bearing has four permanent magnets NdFeB (N38, $B_r = 1.23$ T, $H_c = 963800$ A/m) installed in holes of the stator yoke (Fig. 2), while the 8-pole magnetic bearing has four permanent magnets installed in holes of the stator poles (Fig. 3). For both variants, permanent magnets are magnetized along its shortest edges.

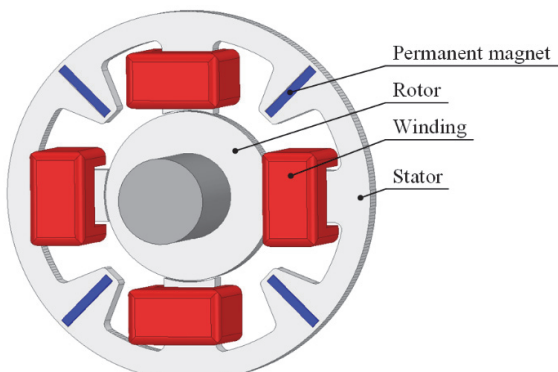


Fig. 2. Structure of the 4-pole radial magnetic bearing

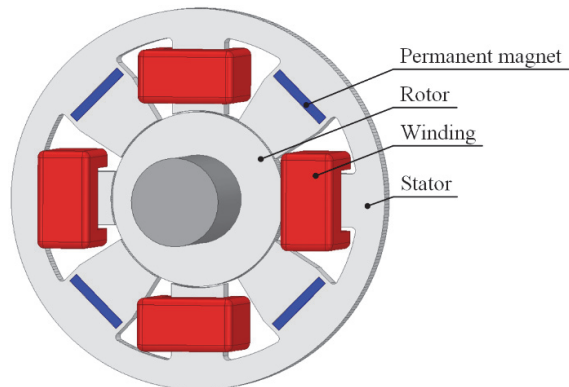


Fig. 3. Structure of the 8-pole radial magnetic bearing

In Table 1. are listed the main geometrical parameters that are common for both versions of magnetic bearings.

Table 1. Parameters of radial magnetic bearings

Parameter	Value
Stator outer radius, r_{s1}	43 mm
Stator inner radius, r_{s2}	20 mm
Stator length, l	10.0 mm
Rotor outer radius, r_{r1}	19.7 mm
Stator pole width, w_p	12.0 mm
Permanent magnet width, w_{pm}	15.0 mm
Permanent magnet height, h_{pm}	2.0 mm

A similar construction to the 4-pole magnetic bearing (Fig. 2) was described in the work [13] where authors used the stator yoke divided into four elements. As a result of such an operation, permanent magnets are installed between stator yoke elements, therefore leakage of the magnetic flux through magnetic bridges was eliminated. Unfortunately, such construction prevents precise assembly of the stator and can be used for applications where a significant air gap can be used, like canned pumps.

Simulation models

Finite element models were prepared in the Ansys Maxwell 3D software that uses an implementation of the $\vec{T} - \Omega$ method for solving the electromagnetic field. The basic equations for the $\vec{T} - \Omega$ method are following [14]:

$$(1) \quad \nabla \cdot \mu(\vec{T} - \nabla\Omega) = 0$$

$$(2) \quad \nabla \times (\nabla \times \vec{T}) = -\gamma \mu \frac{\partial}{\partial t} (\vec{T} - \nabla\Omega)$$

where μ is the permeability and σ is the conductivity.

The current vector potential \vec{T} is defined by:

$$(3) \quad \vec{j} = \nabla \times \vec{T}$$

while the magnetic scalar potential Ω is defined by:

$$(4) \quad \vec{H} = \vec{T} - \nabla\Omega$$

where \vec{H} is the magnetic field intensity.

Fig. 3 presents a finite element model for the 4-pole magnetic bearing prepared in the Ansys Maxwell 3D software. Lamination of the stator and rotor significantly reduces eddy currents, therefore simulation models take only into account magnetostatic calculations. The simulation model is a 3 dimensional due to the long end-windings in comparison to the length of the stator. Consequently, the end-windings area has a noticeable impact on the magnetic force as well as linkage fluxes.

To limit the number of elements and decrease the simulation time, only half of the real object is simulated. Simulation models were discretised using an adaptive meshing procedure implemented in Maxwell 3D software. The main parameter for this procedure is the value of energy error, which was set to 0,5%.

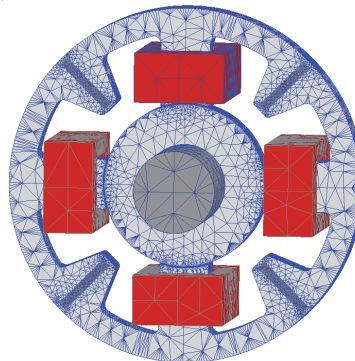


Fig. 3. The finite element model for the 4-pole magnetic bearing

Areas in the vicinity of the permanent magnets and air gap contain a lot of finite elements due to significant changes in the magnetic field.

The simulation model of the 4-pole magnetic bearing contains approx. 260000 finite elements.

A similar simulation model was prepared for the 8-pole magnetic bearing (Fig. 4), which contains approx. 360000 elements. Significantly more finite elements for the 8-pole magnetic bearing result from two times more poles in comparison to the 4-pole magnetic bearing.

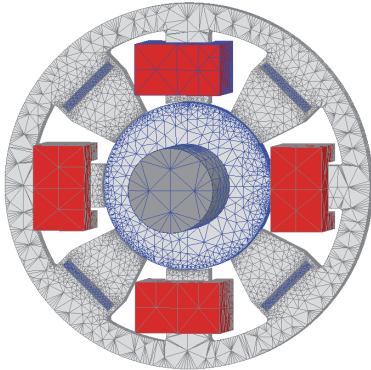


Fig. 4. The finite element model for the 8-pole magnetic bearing

Simulation models were used to calculate the magnetic force and the linkage flux of windings. The magnetic force along the x- and y-axis was calculated from the virtual work method as:

$$(5) \quad F_x = \frac{\partial W_{co}}{\partial x}$$

$$(6) \quad F_y = \frac{\partial W_{co}}{\partial y}$$

where W_{co} denotes the magnetic coenergy.

The flux linkage of windings Ψ_y and Ψ_x are calculated as the sum of the flux linked with coils:

$$(7) \quad \Psi_x = \Psi_1 + \Psi_3 = N\phi_1 + N\phi_3$$

$$(8) \quad \Psi_y = \Psi_2 + \Psi_4 = N\phi_2 + N\phi_4$$

where $\Psi_1, \Psi_2, \Psi_3, \Psi_4$ are the flux linkage of the first, second, third and fourth coil, respectively. N denotes the number of turns. The magnetic flux ϕ_k linked with one turn of wire for the coil is calculated as:

$$(9) \quad \phi_k = \iint_{S_k} \vec{B} \cdot d\vec{S}_k$$

where \vec{B} is the magnetic field density inside the coil and S_k is the cross-sectional area of the coil.

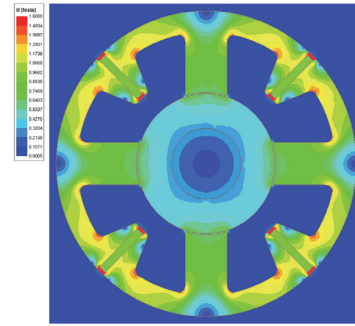
The magnetic force and linkage flux of windings were used to calculate the parameters of magnetic bearings, like the position stiffness k_s , the current stiffness k_i , the initial magnetic force F_{init} , the maximal magnetic force F_{max} , the magnetic force nonlinearity factor h_{non} and the cross-coupling factor h_c , the dynamic inductance L_d , the velocity-induced voltage e_v . All these parameters were thoroughly described in the paper [6].

Results of the magnetic field calculations

Fig. 5.a. and Fig. 5.b. present magnetic field distribution and the normal component to the rotor surface of the magnetic flux density in the air gap for the 4-pole magnetic bearing for the central position of the rotor and lack of the control current. For this working condition the magnetic flux is produced only by permanent magnets and the magnetic field density in the air gap equals 0.65 T.

Fig. 6.a and Fig. 6.b. present magnetic field distribution and the normal component to the rotor surface of the magnetic flux density in the air gap for the 8-pole magnetic bearing for the central position of the rotor and lack of control currents. For this version, the magnetic field density in the air gap equals 0.43 T.

a)



b)

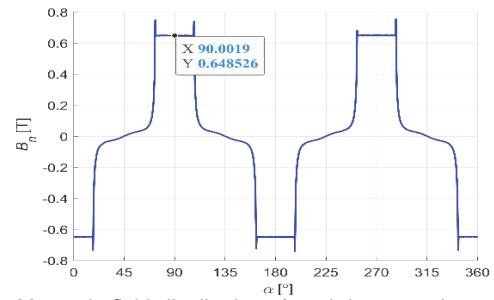
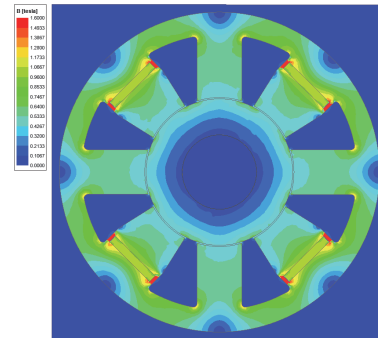


Fig. 5. Magnetic field distribution a) and the normal component to the rotor surface of the magnetic flux density in the air gap b) for the central position of the rotor and the lack of the control current for the 4-pole magnetic bearing

a)



b)

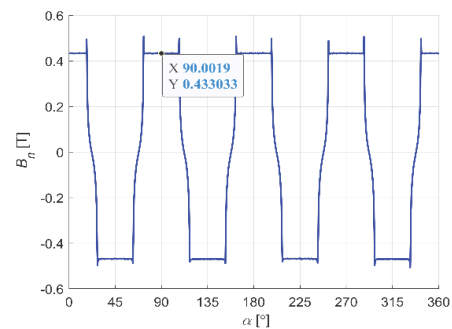


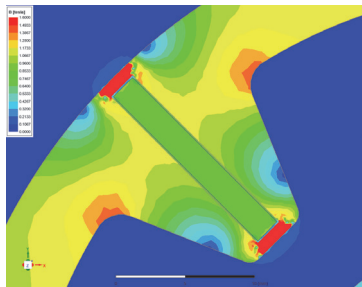
Fig. 6. Magnetic field distribution a) and the normal component to the rotor surface of the magnetic flux density in the air gap b) for the central position of the rotor and the lack of the control current for the 8-pole magnetic bearing

Even though, the same sizes and types of permanent magnets as well as the same cross-sectional area of the stator poles were used for both versions of magnetic bearings, the magnetic flux density inside the stator of the 8-pole magnetic bearing is significantly lower. This is because, for the 8-pole magnetic bearing the magnetic flux generated by the permanent magnet splits into two paths.

The stack of the stator core is fabricated from 20 lamination steels. One lamination is made of one element to

precisely fabricate the stator because the air gap between the stator and rotor equals $300\ \mu\text{m}$. Therefore, both magnetic bearings have a short-circuit of the magnetic flux in the area of the permanent magnets through bridges (Fig. 7).

a)



b)

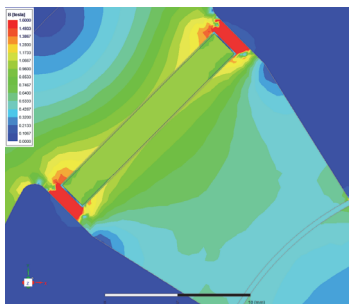
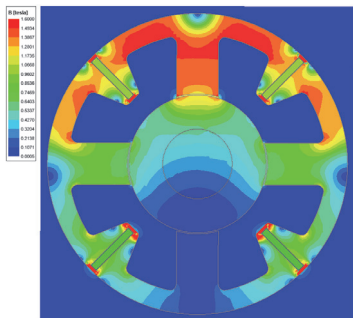


Fig. 7. Zoom of the magnetic field distribution in the area of the permanent magnet for the 4-pole magnetic bearing a) and for the 8-pole magnetic bearing b).

For the 4-pole magnetic bearing total magnetic flux produced by the permanent magnet equals $63.68\ \mu\text{Wb}$, while the amount of the magnetic flux that goes through the short-circuit equals $18.85\ \mu\text{Wb}$ which constitutes 29.6% of the flux produced by the permanent magnet. For the 8-pole magnetic bearing total magnetic flux produced by the permanent magnet equals $69.63\ \mu\text{Wb}$, while the amount of the magnetic flux that goes through the short-circuit equals $18.27\ \mu\text{Wb}$ which constitutes 26.2% of the flux produced by the permanent magnet.

a)



b)

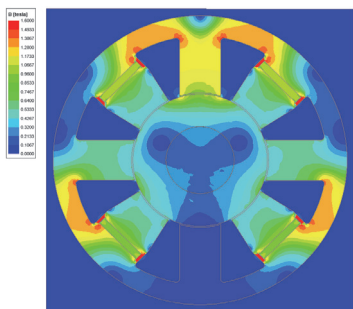
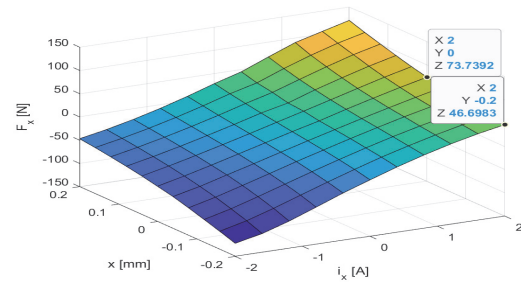


Fig. 8. Magnetic field distribution for the 4-pole magnetic bearing a) and for the 8-pole radial magnetic bearing b) for the central position of the rotor and the control current i_{cy} equals 2 A.

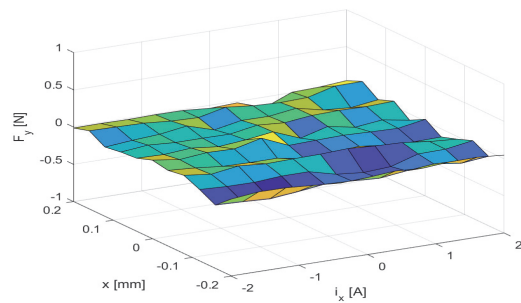
Fig. 8.a and 8.b present magnetic field distribution for the central position of the rotor and the maximal value of the control current for the y-axis. For these working conditions, magnetic bearings generate the maximal value of the magnetic force. For the central position of the rotor and the control current i_{cy} equals 2 A, the 4-pole magnetic bearing generates maximal force F_{max} equals 73.74 N, while the 8-pole magnetic bearing generates maximal force F_{max} equals 40.29 N.

The maximum value of control current is assumed when magnetic field density in the air gap between the lower pole and the stator (for the y-axis) equals zero. Further increase of the control current will increase the value of the magnetic flux in the air gap but in the opposite direction.

a)



b)



c)

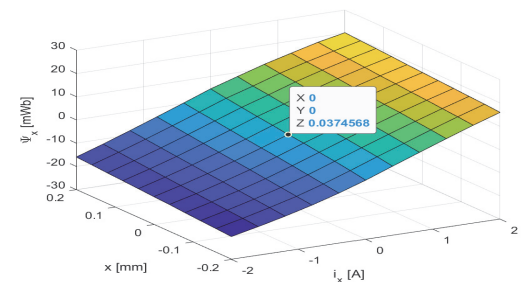


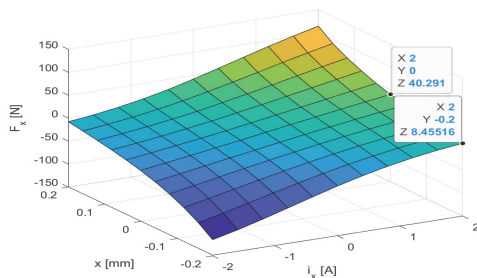
Fig. 9. The magnetic force along the x-axis a), the magnetic force along the y-axis b), the linkage flux of the control winding x c) in the function of the rotor position x and the control current i_x for the 4-pole magnetic bearing

Fig. 9.a, 9.b and 9.c present magnetic force along the x-axis a), magnetic force along the y-axis b) and the linkage flux of control winding for the x-axis c) in the function of the rotor position along the x-axis and the control current i_x for the 4-pole magnetic bearing. These characteristics are presented only for the x-axis, because they are the same for the y-axis. It can be seen that the characteristic of the magnetic force F_x in the function of the rotor position along the x-axis and the control current i_x is almost linear. As well, from this characteristic, we can get information about the maximal and the initial magnetic force generated by the magnetic bearing. It can be seen from Fig. 9.b that there is no cross-coupling between axes because the magnetic force F_y in the function of the rotor position along the x-axis

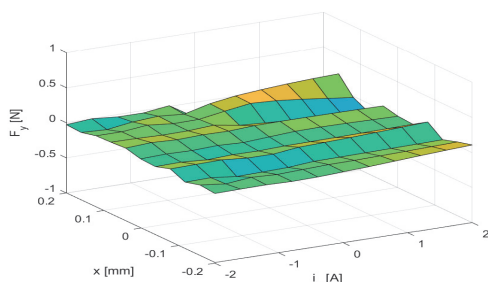
and the control current i_x is almost equal to zero. For the central position of the rotor and lack of the control current, the flux linkage of the control winding equals almost zero (Fig. 9.c). This is because two coils are connected in series and the negative terminal of the first coil is connected with the positive terminal of the second coil.

Fig. 10.a, 10.b and 10.c present magnetic force along the x-axis a), magnetic force along the y-axis b) and the linkage flux of control winding for the x-axis c) in the function of the rotor position x and the control current i_x for the 8-pole radial magnetic bearing. Similarly to the previous version of the magnetic bearing, characteristics are presented only for the x-axis, because they are the same for the y-axis. Also, we can reach the same conclusions as for the 4-pole magnetic bearing.

a)



b)



c)

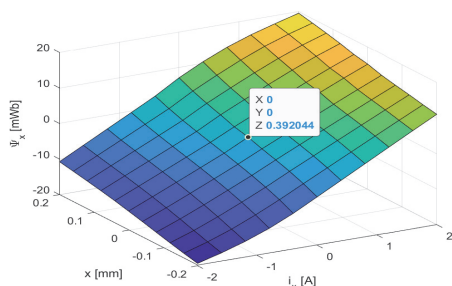


Fig. 10. The magnetic force along the x-axis a), the magnetic force along the y-axis b), the linkage flux of the control winding x c) in the function of the rotor position x and the control current i_x for the 8-pole magnetic bearing

Table 2. Parameters of the 4-pole and 8-pole magnetic bearings

Parameter	Values for the 4-pole magnetic bearing	Values for the 8-pole magnetic bearing
Position stiffness, k_s	123.08 N/mm	150.70 N/mm
Current stiffness, k_i	38.39 N/A	20.91 N/A
Initial force, F_{init}	46.69 N	8.46 N
Maximal force, F_{max}	73.74 N	40.29 N
Force nonlinearity factor, h_{non}	4.19 N	6.46 N
Force cross-coupling factor, h_c	0.05 N	0.06 N
Dynamic inductance, L_d	9.87 mH	8.02 mH
Velocity-induced voltage, e_v	20.50 Vs/m	27.52 Vs/m

Tab. 2 presents the parameters of the 4-pole and 8-pole magnetic bearings obtained from the simulations. It can be seen that the 4-pole magnetic bearing has favourable parameters because it has higher values of current stiffness, initial force, and maximal force. Simultaneously, this version has lower values of position stiffness, force nonlinearity factor as well as force cross-coupling factor.

Conclusions

The paper presents two new constructions of magnetic bearings with permanent magnets. Both versions have four permanent magnets, but for the 4-pole magnetic bearing, permanent magnets are installed in the stator yoke, while for the 8-pole magnetic bearing, permanent magnets are installed in the stator poles. The placement of permanent magnets has a significant impact on the magnetic bearing parameters and as can be seen from Table 2, the 4-pole magnetic bearing has much more favourable parameters than the 8-pole magnetic bearing.

Author: dr hab. inż. Dawid Wajnert, Politechnika Opolska, Katedra Elektrotechniki i Mechatroniki, ul. Prószkowska 76, 45-758 Opole, email: d.wajnert@po.edu.pl

REFERENCES

- [1] Mystkowski A., Energy saving robust control of active magnetic bearings in flywheel, *Acta Mechanica et Automatica*, Vol.6 (2012), No.3, 72-76.
- [2] Kozanecka D., Kozanecki Z., Łagodziński J., Active magnetic damper in a power transmission system, *Communications in Nonlinear Science and Numerical Simulation*, 16 (2011), No. 5, 2273-2278.
- [3] Sikora M., S., Piłat A., K., Numerical model of the axial magnetic bearing with six cylindrical poles, *Archives of Electrical Engineering*, Vol. 68 (2019), 195-208.
- [4] Mystkowski A., Ambroziak L., Investigation of passive magnetic bearing with halbach-array, *Acta Mechanica et Automatica*, Vol.4 (2010), No.4, 78-82.
- [5] Falkowski K., Henzel M., High Efficiency Radial Passive Magnetic Bearing, *Solid State Phenomena*, 164 (2010), 360-365.
- [6] Wajnert D., Comparison of two constructions of hybrid magnetic bearings, *Przegląd Elektrotechniczny*, 95 (2019), No. 12, 53-59.
- [7] Ji L., Xu L., Jin Ch., Research on a Low Power Consumption Six-Pole Heteropolar Hybrid Magnetic Bearing, *IEEE Transactions on Magnetics*, 49 (2013), No. 8, 4918-4926.
- [8] Wu L., Wang D., Su Z., Wang K., Zhang X., Analytical Model of Radial PM biased Magnetic Bearing with Assist Poles, *IEEE Transactions on Applied Superconductivity*, Vol. 26 (2016), No. 7, 0610105.
- [9] Xu S., Sun J. Decoupling Structure for Heteropolar Permanent Magnet Biased Radial Magnetic Bearing With Subsidiary AirGap, *IEEE Transactions on Magnetics*, Vol. 50 (2014), No. 8, 8300208.
- [10] Wajnert D., Analysis of the cross-coupling effect and magnetic force nonlinearity in the 6-pole radial hybrid magnetic bearing, *International Journal of Applied Electromagnetics and Mechanics*, Vol. 61 (2019), 43-57.
- [11] Tomczuk B., Koterka D., Waindok A.: The influence of the leg cutting on the core losses in the amorphous modular transformers, *COMPEL: the International Journal for Computation and Mathematics in Electrical and Electronic Engineering*, Vol. 34 (2015), No. 3, pp. 840-850.
- [12] Schweitzer G., Maslen H., *Magnetic bearings, theory, design, and application to rotating machinery*, Springer, 2009.
- [13] Okada Y., Sagawa K., Suzuki E., Kondo R., Development and Application of Parallel PM Type Hybrid Magnetic Bearings, *Journal of System Design and Dynamics*, Vol. 3 (2009), No. 4, 530-539
- [14] Nakata T., Takahashi N., Fujiwara K., Okada Y., Improvements of the T - Ω method for 3-D eddy current analysis, *Transactions on Magnetics*, Vol. 24 (1988), No. 1, pp. 94-97.